World Academy of Science, Engineering and Technology
International Journal of Electrical and Computer Engineering
Vol:10, No:4, 2016

Research on Axial End Flux Leakage and Detent Force of Transverse Flux PM Linear Machine

W. R. Li, J. K. Xia, R. Q. Peng, Z. Y. Guo, L. Jiang

***Abstract*—**According to 3D magnetic circuit of the transverse flux PM linear machine, distribution law is presented, and analytical expression of axial end flux leakage is derived using numerical method. Maxwell stress tensor is used to solve detent force of mover. A 3D finite element model of the transverse flux PM machine is built to analyze the flux distribution and detent force. Experimental results of the prototype verified the validity of axial end flux leakage and detent force theoretical derivation, the research on axial end flux leakage and detent force provides a valuable reference to other types of linear machine.

***Keywords*—**Transverse flux PM linear machine, flux distribution, axial end flux leakage, detent force.

I. Introduction

COMPARED to rotating electrical machinery, linear machine has no mechanical moving components [1], [2], and transverse flux structure is adapted in transverse flux permanent magnet linear machine (TFPMLM) for improving its mechanical characteristics [3]. Due to the application of axial lamination structure which is similar to rotating electrical machine, TFPMLM features low cost and simple processing technique. Therefore, it is widely used in high frequency and short stroke linear reciprocating motion condition such as thermoacoustic electric generation system (TAEGS).

Axial end effect is generated by precipitous-changed air-gap permeance, which is induced by core breaking of linear machine. Thus, a series of additional effects caused by axial end effect are exist as well, such as axial end flux leakage and detent force. As the structure of transverse flux PM linear machine is dissimilar with the linear counterpart, there is a fundamental difference in the flux distribution.

Majority of researches have analyzed flux leakage using finite element method at present [4]-[9], where had ignored flux leakage variation discipline of machine's end while moving reciprocally. A nonlinear magnetic circuit model has been built in [10], and the conclusion has been found, which the generations of end effect and detent force were attributed to the irregularity of magnetic field distribution inside a motor. Linear flux function on the end of stator core has been proposed in [11], on the basis of which, detent force of the end could be calculated. Permanent magnet end effect has been equivalent to end edge effect in [12], then Schwarz-Christoffel transformation was utilized to calculate the electromagnetic field and an undetermined variable was introduced as an amendment in the calculation of flux density. The method of equivalent magnetic circuit has been used to calculate the flux leakage of permanent magnet cursor linear motor in [13]. Researches within the field of TFPMLM mainly focus on the improvement of topology and technology nowadays, as to axial end flux leakage mainly on the qualitative analysis [14]. The air-gap flux distribution of free-piston transverse flux permanent magnet linear generator has been calculated by the conformal transformation method after PM was equivalent to the surface current model in [15]. Flux leakage inside the free-piston TFPMLM was acquired through the equivalent magnetic network method in [16]. According to the complicated flux leakage distribution of the end, the calculation method of TFPMLM axial end flux leakage is different from that of traditional linear machine. Finite element computation period of TFPMLM takes too much time on account of its particular three-dimensional magnetic circuit structure, thus it is necessary to calculate the end flux leakage rapidly and accurately through numerical method.

In this paper, the area of TFPMLM end flux leakage is divided into several zones, and analytical expression of end flux leakage is derived, on the basis of which, Maxwell stress tensor is used to solve detent force of TFPMLM.

II. Structure and Flux Path of TFPMLM

The structure and diagrammatic cross-section of TFPMLM are illustrated in Fig. 1. Two rows of radial-magnetized permanent magnets are mounted along the axial direction on the mover to provide excitation magnetic field, and the number of permanent magnets in each circumferential row is equal to that of the stator teeth. In order to illustrate easily, the armature winding and the mover shaft are ignored in Fig. 1 (b). To solve the deficiencies in traditional reciprocating oscillation motor such as complex structure and low mechanical strength, axial core lamination structure is adapted, which is similar to conventional electrical rotating machinery and features low cost and simple processing technique.

The main flux drills through the stator core via air-gap and travels along the core lamination till magnetic circuit is formed. Apart from flux leakage between permanent magnets below the core air-gap, permeate flux leakage and end flux leakage hold a dominant position in TFPMLM [17]. As the diminishment of core magnetic resistance adjacent to the q-axis leading flux travel vertically across the lamination air-gap, permeate flux leakage exists between the laminations. The magnetic circuit formed by permanent magnets in the end zone consists of 3 paths, those with transverse flux leakage across the circumferential permanent magnets on the mover, those with axial end flux leakage, and those with self-coupling

W. R. Li is with the Electrical Engineering Institute, Shenyang University of Technology, Shenyang, China (e-mail: sut_li@163.com).

flux leakage through permanent magnets together with air. Traveling via end air-gap along axial direction to stator core, then circulating paralleled with the lamination due to the increase of axial additional air-gap reluctance, the magnetic circuit of axial end flux leakage is circulated from mover permanent magnet flux to stator core.

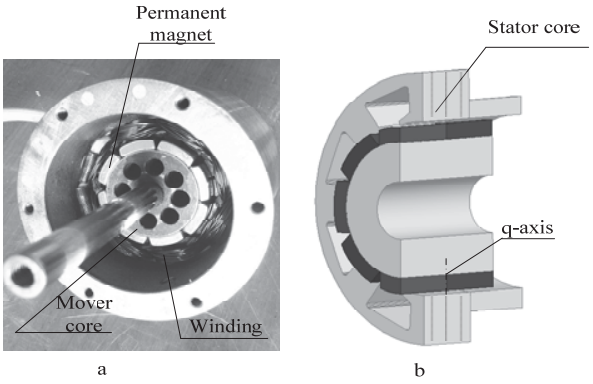

Fig. 1 Structure of TFPMLM

III. End Flux Leakage Distribution and Detent Force

The distribution of end flux leakage is derived according to the comparison of all the possible magnetic circuit length. Division of end flux leakage region is shown in Fig. 2.

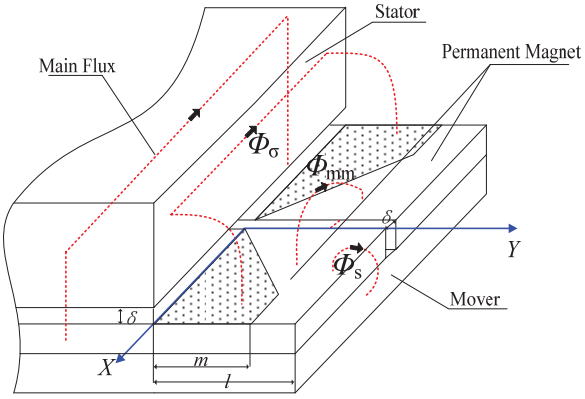

Fig. 2 Region division of end leakage flux in TFPMLM

On the basis of Arc-Line flux path and equivalent reluctance model, the magnetic circuit length of a certain point A on the magnet surface coordinated at (x, y) forming different end flux leakage are as:

$$\begin{cases} l_\sigma = 2\delta + \pi y \\ l_{mm} = 2\delta_{\text{mm}} + \pi x \\ l_s = 2\delta + \frac{3}{2}\pi y \end{cases} \quad (1)$$

where l_σ, l_{mm} and l_s are the length of equivalent magnetic circuit of the axial end flux leakage, the transverse adjacent flux leakage, and the self-coupling flux leakage of permanent magnet respectively, δ is the length of air-gap of linear machine as well as that between transverse permanent magnets, l is the length of emerged magnet or PM position. Boundaries of leakage zones can be drawn by comparing the length of l_σ, l_{mm} and l_s, on this account the scope of axial end flux leakage is ensured subsequently.

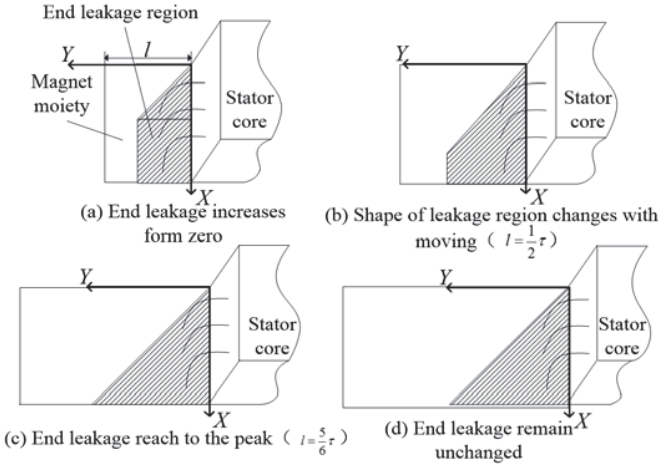

Fig. 3 Diagram of axial end flux leakage

Schematic diagram of end leakage zone changed with the mover position. As shown in Fig. 3, end flux leakage is approximately equal to zero when permanent magnets under the stator core entirely (l=0). The proportion of axial end leakage in total end leakage rises when magnets housed on the mover move left gradually ($l < \frac{\tau}{2}$), as presented in Fig. 3 (a). The total end flux leakage increases accompanied by advance of end flux leakage proportion which is between two adjacent magnets (Φ_{mm}) while the mover moving left, as shown in Fig. 3 (b). Axial end flux leakage (Φ_σ) reaches to the peak when l is equal to $\frac{5}{6}\tau$ (see Fig. 3 (c)), and axial end flux leakage remains unchanged with the movement of the mover subsequently, as shown in Fig. 3 (d). The moving direction is reversed when the mover limiting position is arrived, and the end flux leakage decreases gradually in the return.

The permeance of soft magnetic material Λ is as:

$$\Lambda = \frac{\mu A}{l_m} \quad (2)$$

where, μ is magnetic permeability, A and l_{m} are the sectional area and magnetization length of the soft magnetic material respectively.

According to the analysis of end flux leakage zone, the axial end flux leakage which is created by PMs on the mover (see the shadow region in Fig. 4) drills the stator vertically then spreads transversely through the lamination, and the sectional area of axial end flux leakage is:

$$A=\int_{\frac{2}{5}l}^{l}(\mathrm{x}+\frac{\tau}{2}-l)dx \tag{3}$$

On the basis of Arc-Line flux path permeance model, axial end flux leakage path which passes through the stator end is shown as the arc dashed line in Fig. 4. The radius of the arc is *x*. The magnetic circuit length of the stator core is neglected as the magnetic resistance of which is very small. Considering the magnetic resistance of air-gap and end flux leakage, the circuit length of axial end flux leakage is

$$l(x)=\pi x+2\delta \tag{4}$$

The resistance of axial end flux leakage can be attained through (2)-(4)

$$R_\sigma(x)=\frac{1}{\mu_0}[\frac{\pi}{\left[\frac{3}{5}x+(\frac{\tau}{2}-x)\cdot\ln\frac{5}{2}\right]}+\frac{2\delta}{(\frac{3}{10}\tau x-\frac{9}{50}x^2)}] \tag{5}$$

In the similar way, the internal resistance of the PMs is

$$R_0(t)=\frac{h}{\mu(\frac{3}{10}\tau l-\frac{9}{50}l^2)} \tag{6}$$

According to (5) and (2), the equivalent magnetic circuit length of TFPMLM's axial end flux leakage $l_{\sigma eq}$ can be derived indirectly through magnetic resistant method,

$$l_{\sigma eq}=\mu R_\sigma A=\frac{\pi(\frac{3}{10}\tau l-\frac{9}{50}l^2)}{\left[\frac{3}{5}l+(\frac{\tau}{2}-l)\cdot\ln\frac{5}{2}\right]}+2\delta \tag{7}$$

TFPMLM's axial end flux leakage can be analyzed through equivalent magnetic circuit method which contains internal resistance of PMs and axial end leakage resistance of machine. The equivalent circuit is shown as Fig. 4.

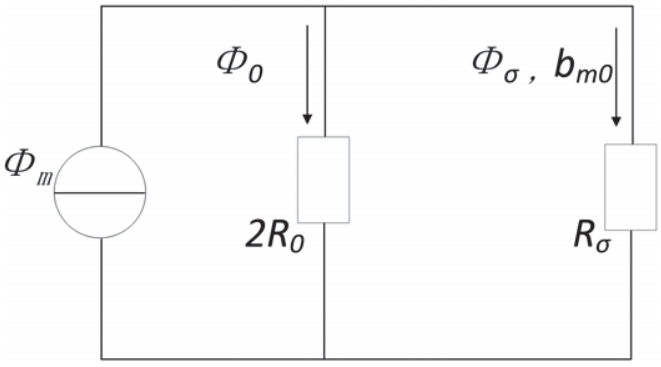

Fig. 4 Equivalent magnetic circuit of axial end flux leakage: where, Φ_m is the total axial end flux leakage generated by the end PMs, b_m is the per unit value of axial end flux leakage induction intensity, B_r is the remanence of the end PM.

The axial end flux leakage can be attained by

$$\Phi_\sigma=b_m B_r A \tag{8}$$

The working point of PMs in end leakage zone can be derived through attainment of b_m.

$$b_m=\frac{2R_0}{R_\sigma+2R_0}=\frac{2h}{l_{\sigma eq}+2h} \tag{9}$$

The axial end flux leakage can be attained through (8) and (9)

$$\Phi_\sigma(x)=h_m B_r A=\frac{B_r(\frac{3}{10}\tau l-\frac{9}{50}l^2)}{1+\frac{\pi(\frac{3}{10}\tau l-\frac{9}{50}l^2)}{\left[\frac{3}{5}l+(\frac{\tau}{2}-l)\cdot\ln\frac{5}{2}\right]}+2\delta} \tag{10}$$

where R_σ is end reluctance; μ_0 is air permeability; δ is air gap length; τ is polar distance; Φ_σ is end flux leakage; h_m is permanent magnet working point; Br is permanent magnet remanence; h is thickness of permanent magnet.

Base on the derivation above, the normal force density of the stator end σ_m is as

$$\sigma_m=\frac{B^2{}_\sigma}{2\mu_0}=\frac{\Phi^2{}_\sigma}{2\mu_0 A^2} \tag{11}$$

Assuming rightward detent force as positive, the detent force of the leftside PMs on the mover can be obtained by

$$F_{\mathrm{L}}(t)=\int\sigma_m\mathrm{d}s=\frac{\Phi_\sigma^2}{2\mu_0 s}$$
$$=B_r^2(\frac{3}{10}\tau l-\frac{9}{50}l^2)(\frac{\pi(\frac{3}{10}\tau l-\frac{9}{50}l^2)+2\delta\left[\frac{3}{5}l+(\frac{\tau}{2}-l)\cdot\ln\frac{5}{2}\right]}{\pi(\frac{3}{10}\tau l-\frac{9}{50}l^2)+2(\delta+h)\left[\frac{3}{5}l+(\frac{\tau}{2}-l)\cdot\ln\frac{5}{2}\right]})^2 \tag{12}$$

In the same way, considering the impact of rightside PMs' detent force on the mover has a tendency of leftward moving, detent force of the rightside PM can be obtained through substitution of *l-x* in (12), which is negative correspondingly.

IV. Analysis on Practical Example

The aforementioned analytical method is implemented on division of leakage zones in a TFPMLM prototype, the basic parameters concerning axial end leakage model of the prototype are presented in Table I.

Three-dimensional finite element model is constructed on the basis of related parameters of TFPMLM (see Fig. 5).

TABLE I
PARAMETERS OF TFPMLM

Parameter[unit]	Value
Air-gap/ Air-gap between PMs (δ) [mm]	0. 8
Range of l[mm]	3~12
Polar arc (τ) [mm]	11.5
Thickness of PM (h) [mm]	4
Amplitude of velocity (v) [m/s]	4.7
Frequency of driving force (f) [Hz]	100

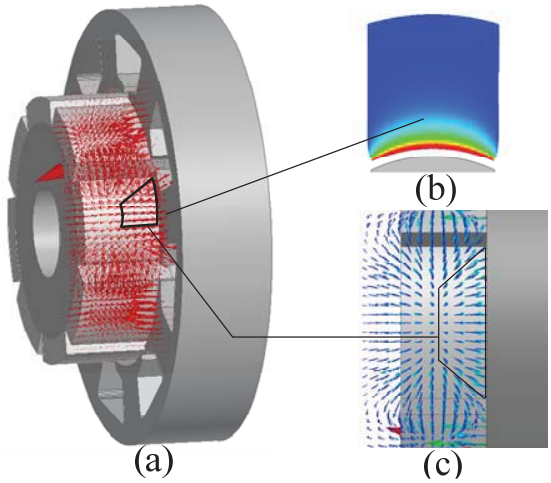

Fig. 5 Diagram of TFPMLM's flux distribution

The vector-graph of the magnetic induction intensity in TFPMLM with no load is shown in Fig. 5 (a). Through air-gap, tooth and yoke of the stator, the main flux of TFPMLM drills into the corresponding magnet and the magnetic circuit plane is composed simultaneously, which is orthogonal to the moving direction, and there apparently exists flux leakage on the end, as shown in Fig. 5 (c). The distribution cloud chart and path diagram are depicted in Figs. 5 (b) and (c) respectively in order to check the property of axial end leakage distribution more clearly. What can be seen from the diagrams is that the end flux leakage owns three flux paths, the boundary between the axial end leakage and the flux leakage of end PMs can be regarded as $y=x$ according to the division of leakage zones, and the axial end leakage shown as the box with solid line in Fig. 5 (c) gets into the stator core end vertically, then travels along the adjacent magnet because of the existence of air-gap sandwiched between the stator lamination, which certifies the paths and zones of end flux leakage is consistent with the theoretical analysis.

According to the parameters of TFPMLM, the result of axial end flux leakage using numerical method is attained. The corresponding curve comparison through integration of stator end magnetic induction intensity using FEM is attained, as shown in Fig. 6.

According to Fig. 6, half period of the comparison results between FEM and numerical method are taken, as FEM has a disadvantage of long period of calculation. The axial end flux leakage comparisons are plotted with end flux leakage as ordinate against PM position (emerge length) as abscissa. Within the travel range of 3mm to 12mm, the axial end flux leakage increase with the advance of PM position/length and flux leakage area. The axial end flux leakage tends to be stable at 1.72T when the PM position is 9.6mm. There is slight deviation between the result of FEM and numerical method. The same trend shows validity of the axial end flux leakage numerical method.

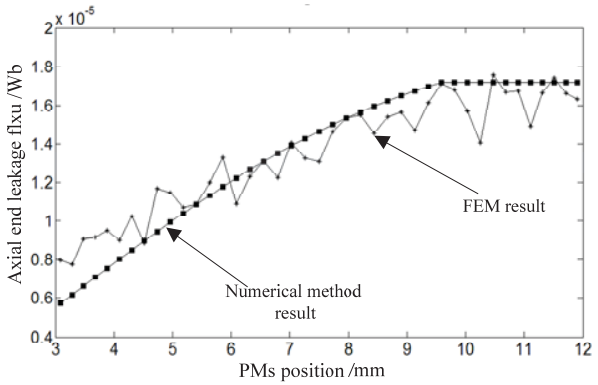

Fig. 6 Axial end flux leakage under different PM position

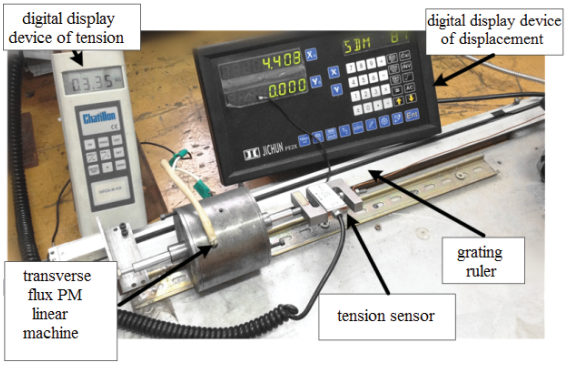

Fig. 7 Measurement system of detent force in TFPMLM

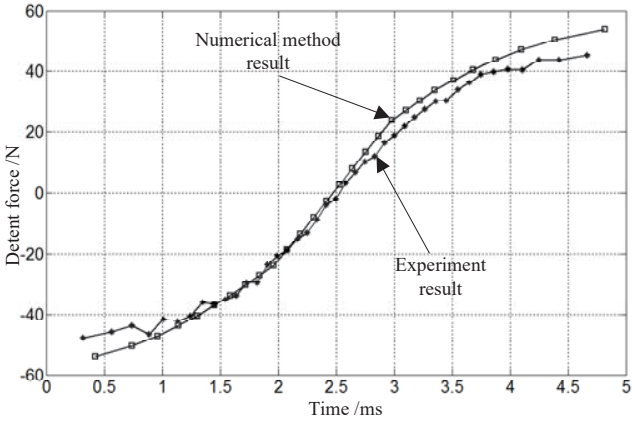

Fig. 8 Detent force of TFPMLM

Detent force is the direct reflection of the axial end flux leakage in TFPMLM. The measurement system is built to measure the detent force in TFPMLM as shown in Fig. 7. The measurement system consists of detection module and display module, which typically includes the grating ruler, the digital

display device of displacement, the digital display device of tension and the tension sensor. The relative displacement of the mover is detected by the grating ruler and shown in the digital display device, and the end detent force of different emerged positions can be detected by the tension sensor simultaneously.

The comparison on experimental results and theoretical calculating results of end detent force with different PM position *l* is presented in Fig. 8. The detent force comparison between experiment and theoretical derivation are plotted with detent force as ordinate against time by conversion as abscissa. According to Fig. 8, the amplitude of the detent force by FEM and numerical calculation are 45.6N and 53.2N correspondingly. The results prove that running frequency of the linear machine keeps in same with that of detent force. According to the analysis, detent force has a controversy phase with that of mover's position, thus produces restoring action which is similar to the mechanical spring.

V. Conclusion

This paper analyzes the magnetic circuit length of TFPMLM's end region, and divides end flux leakage region into three zones. The distribution and range of the axial end flux leakage is ascertained. The amount and distribution discipline of axial end flux leakage in different end positions are acquired according to the end PMs working point calculation, thus the function of TFPMLM axial flux leakage with end position in end region is derived. Base on the derivation above, detent force of linear machine is acquired through Maxwell stress tensor. Experimental results of the prototype together with the FEM simulation verify the validity of axial end flux leakage and detent force theoretical derivation.

References

[1] Trung Kien Hoang, Do Hyun Kang, Ji Young Lee. Comparisons Between Various Designs of Transverse Flux Linear Motor in Terms of Thrust Force and Normal Force (J). IEEE Transactions on magnetics, 2010, 46(10):3795-3801.

[2] Ji Bin Zou, Qian Wang, Yong Xiang Xu. Influence of the Permanent Magnet Magnetization Length on the Performance of a Tubular Transverse Flux Permanent Magnet Linear Machine Used for Electromagnetic Launch (J). IEEE Transactions on plasma science, 2011, 39(1): 241-246.

[3] Yong Ming Xia, Qin Fen Lu, Yun Yue Ye, et al. Novel Flux Reversal Linear Oscillatory Motor with Two Divided Stators (J). Proceedings of the CSEE, 2007, 27(27): 104-107.

[4] Jia Kuan Xia, Cheng Yuan Wang, Hao Dong Li, et al. Study of End-Effects Analysis and NN Compensation Technique of Linear Motor for High Precision NC Machine (J). Proceedings of the CSEE, 2003, 23(8): 100-104.

[5] Kai Lin Pan, Jian Zhong Fu, ZiChen Chen. Detent Force Analysis and Reduction of PMLSM (J). Proceedings of the CSEE, 2004, 24(4): 112-115.

[6] Zhu Z Q, Xia Z P, Howe D, et al. Reduction of cogging force in slotless linear permanent magnet motors (J). IEE Proceedings Electric Power Applications, 1997, 144(4): 277-282.

[7] Yu Wu Zhu, Sang Gun Lee, Koon Seok Chung, et al. Investigation of Auxiliary Poles Design Criteria on Reduction of End Effect of Detent Force for PMLSM (J). IEEE Transactions on Magnetics, 2009, 45(6):2863-2866.

[8] Yue Tong Xu, Jian Zhong Fu, Zi Chen Chen. Thrust Ripple Optimization and Experiment for PMLSM (J). Proceedings of the CSEE, 2005, 25(12): 122-126.

[9] Qin Fen Lu, Yun Yue Ye. A Study on Characteristic of Moving Magnet Type Linear Oscillatory Motor (J). Proceedings of the CSEE, 2005, 25(19):135-139.

[10] Hao Wang, Zhi Jing Zhang, Cheng Ying Liu. Compensation Methods of Longitudinal End Effects in Permanent-magnet Linear Synchronous Motor (J). Proceedings of the CSEE, 2010, 30(15): 58-63.

[11] Bing Peng, Tie Fa Liu, Nan Zhang, et al. A Method for Reducing the End Effect Force Fluctuation by the Concave Profile End-tooth in Permanent Magnet Linear Motors (J). Transactions of China Electrotechnical Society. 2015, 30(7): 119-124.

[12] Ming Na Ma. Research on End Effects for Multi-Segment Permanent Magnet Linear Synchronous Motor (D). China: Harbin Institute of Technology, 2014.

[13] Wen Long Li, K. T Chau, Chun Hua Liu, et al. Analysis of Tooth-Tip Flux Leakage in Surface-Mounted Permanent Magnet Linear Vernier Machines (J). IEEE Transactions on Magnetics, 2013, 49(7):3949-3952.

[14] Qian Wang. Study on Electromagnetic Field and Electromagnetic Force of Tubular Transverse Flux Permanent Magnet Linear Machine (D). China: Harbin Institute of Technology: 2010.

[15] Alija Cosic, C. Sadarangani. Cogging Torque Calculations for a Novel Concept of a Transverse Flux Linear Free-Piston Generator. Proceedings of International Conference on Linear Drives and Industry Applications (C). Kobe-Awaji, Japan, 2005.

[16] W. M. Arshad, P. Thelin, C. Sadarangani, et al. Analytical Analysis and Dimensioning of a Low-Leakage Linear Transverse-Flux Machine (C). Proceedings of International Conference on Power Electronics, Machines and Drives. Edinburgh, UK, 2004: 414-419.

[17] Jia Kuan Xia, Wen Rui Li, Xin He, et al. Analysis of Anisotropic Permeate Leakage Flux on Transverse Flux Permanent Magnet Linear Machine (J). Transactions of China Electrotechnical Society. 2015, 30(14): 518-524.